Kiatkittikul *et al.*
European Journal of Hybrid Imaging (2023) 7:23
https://doi.org/10.1186/s41824-023-00176-3

European Journal of Hybrid Imaging

ORIGINAL ARTICLE Open Access

Head-to-head comparison of ^{18}F-FDG and ^{18}F-FES PET/CT for initial staging of ER-positive breast cancer patients

Peerapon Kiatkittikul[1*], Supanida Mayurasakorn[1], Chetsadaporn Promteangtrong[1], Anchisa Kunawudhi[1], Dheeratama Siripongsatian[1], Natdanai Hirata[1], Attapon Jantarato[1], Natphimol Boonkawin[1], Sukanya Yaset[1], Pattanapong Kongsakorn[1], Warunya Phewnual[1] and Chanisa Chotipanich[1]

*Correspondence:
peerapon.kia@cra.ac.th

[1] National Cyclotron and PET Centre, Chulabhorn Hospital, Chulabhorn Royal Academy, 906 Kamphaeng Phet 6 Rd., Lak Si, Bangkok 10210, Thailand

Abstract

Purpose: To compare the diagnostic performance of ^{18}F-fluorodeoxyglucose (^{18}F-FDG) and ^{18}F-fluoroestradiol (^{18}F-FES) positron emission tomography/computed tomography (PET/CT) for initial staging of estrogen receptor (ER) positive breast cancer.

Methods: Twenty-eight patients with ER-positive breast cancer underwent ^{18}F-FDG and ^{18}F-FES PET/CT for initial staging. Diagnostic performance and concordance rates were analyzed for both radiotracers. Semiquantitative parameters of maximum standardized uptake value (SUVmax) and tumor-to-normal ratio (T/N ratio) were compared using Wilcoxon signed-rank test. Factors potentially affecting the degree of radiotracer uptake were analyzed by multi-level linear regression analysis.

Results: The overall diagnostic performance of ^{18}F-FES was comparable to ^{18}F-FDG, except for higher specificity and NPV, with sensitivity, specificity, PPV, NPV, and accuracy of 87.56%, 100%, 100%, 35.14%, and 88.35%, respectively, for ^{18}F-FES and 83.94%, 30.77%, 94.74%, 11.43%, and 95.37%, respectively, for ^{18}F-FDG. Diagnostic performance of strong ER expression was better in ^{18}F-FES but worse for ^{18}F-FDG. There was a correlation of mucinous cell type and Allred score 7–8 with ^{18}F-FES uptake, with correlation coefficients of 26.65 (19.28, 34.02), 5.90 (– 0.005, 11.81), and *p*-value of < 0.001, 0.05, respectively. Meanwhile, luminal B and Ki-67 were related to ^{18}F-FDG uptake, with correlation coefficients of 2.76 (1.10, 0.20), 0.11 (0.01, 0.2), and *p*-value of 0.018, 0.025, respectively.

Conclusion: Diagnostic performance of ^{18}F-FES is comparable to ^{18}F-FDG, but better for strongly ER-positive breast cancer. Combination of ^{18}F-FES and ^{18}F-FDG would potentially overcome the limitations of each tracer with more accurate staging.

Keywords: ^{18}F-FES, ^{18}F-FDG, ^{18}F-fluroestradiol, ^{18}F-flurodeoxyglucose, ER-positive breast cancer, Initial staging

Introduction

Breast cancer is the most common cancer in woman, accounting for 24.2% of all cancers in women, and the most frequent cause of cancer-related death in women, at 15% (Ferlay et al. 2019). The prognosis and management of breast cancer depends on TNM staging and estrogen receptor (ER) expression. Approximately 75% of women with breast cancer have ER-positive tumors (Blamey et al. 2010). The evaluation of ER relies on immunohistochemistry (IHC) testing, which requires tissue biopsy, a more invasive procedure that may not be available in some regions.

Positron emission tomography/computed tomography (PET/CT) is an evaluation tool that is especially useful in cancer patients, providing functional information at the molecular level. ^{18}F-fluorodeoxyglucose (^{18}F-FDG) is a glucose analog that reflect the metabolic activity of the tumor cell. ^{18}F-FDG PET/CT is widely used in the evaluation of various cancers, including breast cancer. However, it has several limitations, such as infection or inflammation, resulting in false-positive lesions (Boellaard et al. 2015).

^{18}F-fluoroestradiol (^{18}F-FES) is an estrogen analog and an FDA-approved radiotracer for PET scans (Research C for DE and Drug Trial Snapshot: CERIANNA 2020). ^{18}F-FES can selectively bind to ER in cancer cells, especially breast cancer, and exhibits a good correlation to the degree of ER expression detected by IHC (Gupta et al. 2017; Mintun et al. 1988). Thus, ^{18}F-FES PET can be used for non-invasive evaluation of the ER in the whole body. This study aimed to compare the diagnostic performance of ^{18}F-FDG and ^{18}F-FES PET/CT in the initial staging of ER-positive breast cancer.

Materials and methods

Study design

This was a retrospective, single-center comparative imaging study, approved by the Human Research Ethics Committee of Chulabhorn Research Institute, with no external source of funding. The primary objective was to compare the diagnostic performance of ^{18}F-FDG and ^{18}F-FES PET/CT in the initial staging of ER-positive breast cancer. The secondary objective was to identify the concordance rate between ^{18}F-FDG and ^{18}F-FES PET/CT, including potential factors affecting the degree of ^{18}F-FDG and ^{18}F-FES uptake.

This study recruited all breast cancer patients who underwent PET/CT scan at National Cyclotron and PET Centre, Chulabhorn Hospital, Bangkok, Thailand, from 1 September 2020 to 31 October 2022. The inclusion criteria were patients aged > 18 years with pathologically confirmed ER-positive breast cancer. The exclusion criteria were those with fasting blood sugar > 200 mg/dL, a history of other cancers, known ER negativity, unknown ER status, and pregnancy or breastfeeding.

The demographic data collection included age, sex, body mass index (BMI), menopausal status, and tissue pathology results. ER expression was defined according to: (i) luminal A (Ki-67 < 14%) and luminal B (Ki-67 > 14%) subtype (Network 2023); and (ii) Allred score calculated from the summation of intensity and proportion scores of ER expression (range, 0–8). The Allred score was further classified as negative (score 0–2), intermediate (score 3–6), or high (score 7–8) (Weischenfeldt et al. 2017).

Imaging protocol

^{18}F-FDG and ^{18}F-FES PET/CT were performed on different days within 2-week interval. The patients were advised to avoid any meals for at least 4–6 h and strenuous exercise for 24 h prior to ^{18}F-FDG PET/CT, while there was no specific preparation for ^{18}F-FES PET/CT. The plasma glucose level was tested before ^{18}F-FDG PET/CT. If higher than 200 mg/dL, ^{18}F-FDG PET/CT was postponed. The intravenous injection dose of ^{18}F-FDG was calculated according to patient's body weight (2.59 MBq/kg), but a fixed dose was used in ^{18}F-FES (111 MBq). After 60-min radiotracer administration, PET scan was acquired from vertex to proximal thigh using a 64-slice Siemens/Biograph Vision PET/CT scanner (Siemens Healthcare GmbH, Erlangen, Germany) in the three-dimensional mode with continuous bed motion method at speed of 1.6–1.8 mm/s. The matrix was 440×440, with the reconstruction methods of True X and Time of Flight. The CT parameters were 120 kV tube voltage, 25 mAs current, and 3 mm slice thickness.

Image analysis

^{18}F-FDG and ^{18}F-FES PET/CT scans were separately interpreted by three board-certified nuclear medicine physicians with consensus. ^{18}F-FDG PET/CT were reviewed by P.K., A.K., and C.P. The ^{18}F-FES PET/CT were reviewed by P.K., D.S., and C.C. The images were reviewed using Syngo.via workstation (Siemens Healthcare GmbH). The physicians were blinded to clinical data at the time of review.

Image analysis was based on visual detection. An area of focal uptake higher than the surrounding background indicated a positive lesion. The lesions were assessed as primary tumor (T stage), regional nodal metastases (N stage), and distant metastasis (M stage) based on the eighth edition of the American Joint Committee on Cancer Staging System for breast cancer (Amin et al. 2017). A maximum of seven lesions were acquired in each region. Regional nodal metastasis was classified into axillary level I, level II, level III, and supraclavicular node. Non-regional node metastasis, brain, visceral organ in the chest and abdomen, bone, and soft tissue involvement were individual sites for distant metastasis.

Three-dimensional voxels of interest (VOI) were drawn around the lesions, with semiquantitative parameters acquired by three designated physicians. The VOIs were manually adjusted by the physicians to avoid false-positive regions caused by normal physiological uptake. The maximum standardized uptake value (SUVmax) was determined in all lesions. The tumor-to-normal ratio (T/N ratio) of all lesions were calculated by dividing SUVmax of the lesion with SUVmean of the mediastinal blood pool.

Reference standard

Tissue histopathology with immunohistochemistry staining is the gold standard for diagnostic accuracy analysis. For non-biopsied lesions, the reference standard was anatomically observed on CT or magnetic resonance imaging (MRI). For nodal metastasis, there was a cluster of at least three size-independent nodes at one site or fewer than three lymph nodes with at least one measuring ≥ 1 cm along the short axis or spherical form or central necrosis. For lung metastasis, a solid pulmonary nodule, reticulonodular pattern, cavitating nodule, or lymphangitis carcinomatosis was included. For

bone metastasis, an osteolytic or sclerotic lesion with cortical breakthrough, periosteal reaction, expansile appearance, or pathological fracture observed by CT or an abnormal marrow signal on MRI were considered. For other distant metastasis, a nodule or mass lesion not compatible with benign lesion was considered.

Statistical analysis

Demographic data from all patients are presented as number, percentage, mean ± SD (standard deviation), or median with interquartile range (IQR). The concordance rates were calculated between both radiotracers. Diagnostic accuracy was defined by sensitivity, specificity, positive predictive value (PPV), negative predictive value (NPV), and accuracy. Differences in semiquantitative parameters were analyzed using Wilcoxon signed-rank test. Potential factors affecting the degree of uptake for both radiotracers were identified by multi-level linear regression analysis. A p-value of < 0.05 was considered statistically significant. STATA software, version 11 (Stata Corp LLC; College Station, TX, USA) was applied for statistical analyses.

Results

Sixty-four patients underwent PET/CT scan of both radiotracers for initial staging in breast cancer. Of these, 13 patients were excluded due to ER negativity, followed by 15 with an indication of complete staging after surgery and 8 of unknown ER status. Thus, 28 female patients were included, most of whom were in menopause (78.57%) and who had a mean age of 59.1 ± 13.23 years, and mostly normal BMI (67.86%) at 22.10 ± 3.29 kg/m^2. In pathological results, 20 patients (71.43%) had invasive ductal carcinoma (IDC), followed by 5 (17.86%) invasive lobular carcinoma (ILC), 1 (3.57%) invasive micropapillary carcinoma, and 1 (3.57%) mucinous carcinoma. The Allred scoring system showed 18 patients with score of 8, followed by 1 (score of 7), 2 (score of 5), 3 (score of 3), and 4 unknown score due to lack of data. For IHC results, 5 (17.86%) were luminal A, followed by 18 (64.28%) luminal B, and 5 unknown due to lack of data (Table 1).

For patient analysis (Table 2), two patients (7.14%) had discordant results between ^{18}F-FDG and ^{18}F-FES PET/CT in T stage. One had falsely downstage from ^{18}F-FDG PET/CT and the other had falsely downstage from ^{18}F-FES PET/CT. In N stage, 7 patients (25%) had discordant results, including 1 falsely upstage from ^{18}F-FDG, 4 falsely downstage from ^{18}F-FDG, and 2 falsely downstage from ^{18}F-FES. In M stage, 6 patients (21.43%) had discordant results, namely 3 falsely upstage in ^{18}F-FDG (all from non-regional reactive nodes), 2 falsely downstage in ^{18}F-FDG (one non-regional lymph node and the other with bone metastases), and 1 falsely downstage in ^{18}F-FES (bone metastasis). In overall TNM stage, 18 patients (64.29%) had concordant results (Fig. 1). Among 10 discordant results, there were 3 false positive of ^{18}F-FDG PET/CT with increased TNM stage, 5 false negative of ^{18}F-FDG PET/CT with decreased TNM stage (Fig. 2), 1 false negative of ^{18}F-FES PET/CT with decreased TNM stage (Fig. 3), and 1 both false positive ^{18}F-FDG and false negative ^{18}F-FES PET/CT (Fig. 4).

In the lesion analysis, there were a total of 206 lesions with 193 lesions of true metastasis. These included 54 T stage, 85 N stage, and 67 M stage. For M stage, there were 20 non-regional lymph nodes, 27 bone lesions, 19 lung lesions, and 1 adrenal

Table 1 Baseline characteristics

Baseline data (28)	Results
Age (mean ± SD)	59.1 ± 13.23
Menopause (n, percent)	
Yes	22 (78.57%)
No	4 (21.43%)
BMI (mean ± SD)	22.10 ± 3.29
Underweight (< 18.5)	1 (3.57%)
Normal (18.5–24.9)	19 (67.86%)
Overweight (25.0–30)	7 (25%)
Obesity (> 30)	1 (3.57%)
Cell type (n, percent)	
Invasive ductal carcinoma (IDC)	20 (71.43%)
Invasive lobular carcinoma (ILC)	5 (17.86%)
Invasive micropapillary carcinoma	1 (3.57%)
Mucinous carcinoma	1 (3.57%)
Allred Score (n, percent)	
3	3 (10.71%)
5	2 (7.14%)
7	1 (3.57%)
8	18 (64.29%)
N/A	4 (14.29%)
Luminal (n, percent)	
A	5 (17.86%)
B	18 (64.28%)
N/A	5 (17.86%)

BMI Body mass index, *N/A* Not applicable, *SD* Standard deviation

gland lesion. ^{18}F-FDG PET detected 171 lesions with true metastasis in 162 lesions. ^{18}F-FES PET detected 169 lesions with true metastasis in all lesions.

The diagnostic performance of ^{18}F-FES PET/CT achieved 87.56% sensitivity, 100% specificity, 100% PPV, 35.14% NPV, and 88.35% accuracy. Meanwhile, the diagnostic performance of ^{18}F-FDG PET/CT exhibited 83.94% sensitivity, 30.77% specificity, 94.74% PPV, 11.43% NPV, and 80.58% accuracy. Further subgroup analysis in strong ER expression group (Allred score of 7–8), there was an increase in diagnostic performance of ^{18}F-FES with 94.95% sensitivity, 100% specificity, 100% PPV, 64.29% NPV, and 95.37% accuracy. In contrast, there was a decrease in diagnostic performance of ^{18}F-FDG with 72.73% sensitivity, 44.44% specificity, 93.51% PPV, 12.9% NPV, and 70.37% accuracy.

The semiquantitative parameters of all lesions showed statistical significance for high T/N ratio of ^{18}F-FES when compared with ^{18}F-FDG, with median (IQR) of 3.335 (1.61–6.38) and 2.635 (1.58–4.79), respectively ($p = 0.016$). However, there was no statistically significant difference in SUVmax of ^{18}F-FES and ^{18}F-FDG, with median (IQR) of 5.28 (2.55–10.60) and 5.68 (3.41–10.03), respectively ($p = 0.646$). For subgroup analysis, ILC cell type, Allred score 7–8, and luminal A category yielded a statistically significant increase degree of ^{18}F-FES uptake in both SUVmax ($p = 0.028$, $p = 0.003$, and $p = 0.019$, respectively) and T/N ratios ($p = 0.015$, $p < 0.001$,

Table 2 TNM staging of ^{18}F-fluorodeoxyglucose and ^{18}F-fluoroestradiol PET/CT

Cases	^{18}F-flurodeoxyglucose PET/CT				^{18}F-fluoroestradiol PET/CT			
	T	N	M	Stage	T	N	M	Stage
1	1	0	0	1	1	0	0	1
2	1	1**	0	2a	1	0	0	1
3	2	1	0	2b	2	1	0	2b
4	4	0*	0*	3b	4	1	1	4
5	2	0	0	2a	2	0	0	2a
6	4	0	1**	4	4	0	0	3b
7	4	1	0	3b	4	1	0	3b
8	4	0	0	3b	4	0	0	3b
9	4	3	1	4	4	3	1	4
10	2	3	1	4	2	3	1	4
11	2	3	1	4	2	3	1	4
12	4	3	1**	4	4	3	0	3c
13	4	3	1	4	4	3	1	4
14	2	1	0*	2b	2	1	1	4
15	3	3	0	3c	3	3	0	3c
16	1	0*	0	1	1	1	0	2a
17	2	3	1**	4	0*	0*	0	0
18	3	2	1	4	3	2	1	4
19	0*	0*	0	0	1	1	0	2a
20	2	0	0	2a	2	0	0	2a
21	2	1	0	2b	2	1	0	2b
22	1	1	0	2a	1	1	0	2a
23	2	0	0	2a	2	0	0	2a
24	2	1	1	4	2	0*	0*	2a
25	2	0*	0	2a	2	1	0	2b
26	2	1	1	4	2	1	1	4
27	2	0	0	2a	2	0	0	2a
28	2	0	0	2a	2	0	0	2a

*False negative lesion, resulting in down staging, ** False positive lesion, resulting in up staging

PET/CT Positron emission tomography/computed tomography

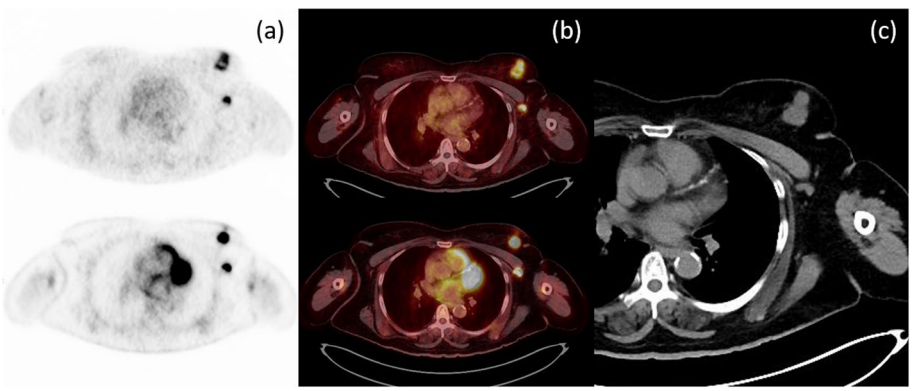

Fig. 1 Axial PET (**a**) and axial fusion (**b**) images of ^{18}F-FES (above) and ^{18}F-FDG (below) with concordant uptake of both radiotracers in a left breast mass and left axillary node metastasis, in correlation with CT imaging (**c**)

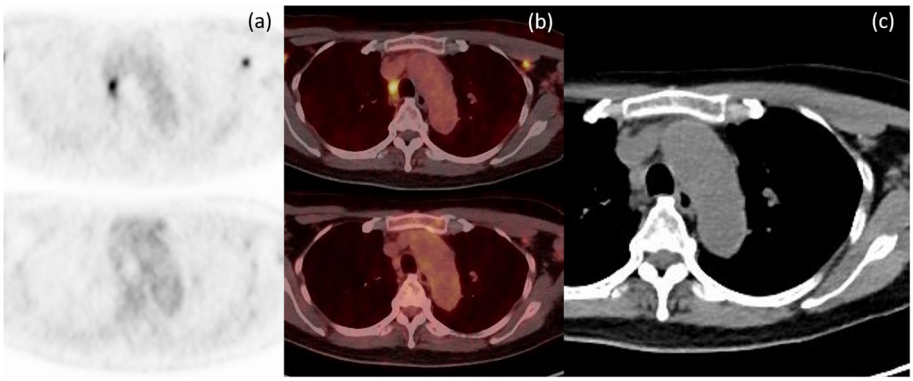

Fig. 2 Axial PET **a** and axial fusion **b** images of ^{18}F-FES (above) and ^{18}F-FDG (below) for ^{18}F-FES-avid enlarged nodes on CT imaging **c** without ^{18}F-FDG avidity at left axillary and right paratracheal nodes

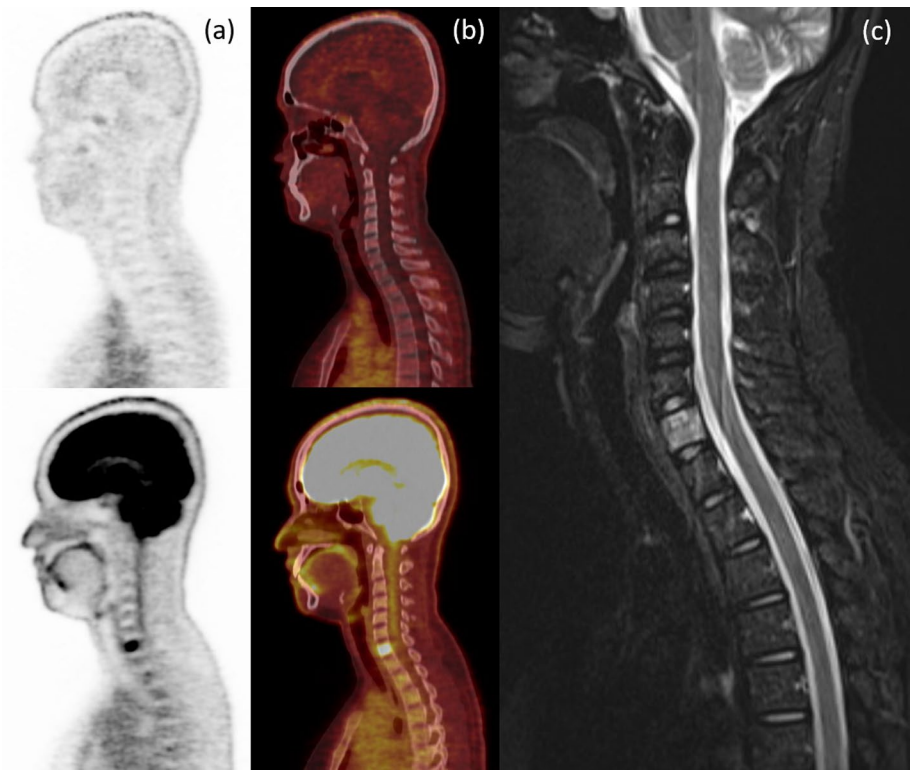

Fig. 3 Sagittal PET **a** and sagittal fusion **b** images of ^{18}F-FES (above) and ^{18}F-FDG (below) for ^{18}F-FDG-avid hyperT2 bone metastasis at C7 vertebra on MRI (**c**) without ^{18}F-FES avidity

and $p = 0.004$, respectively). In contrast, a significant increase in ^{18}F-FDG uptake was noted for Allred score < 7 ($p < 0.001$ for both SUVmax and T/N ratio) and luminal B subtype (p-value = 0.008 for SUVmax) (Table 3).

Several factors significantly affected the degree of ^{18}F-FDG PET in breast cancer. Luminal B subtype and Ki-67 were related to the degree of ^{18}F-FDG uptake with correlation coefficient of 2.76 (95%CI 1.10,11.92), $p = 0.018$ and 0.11 (95%CI 0.01,0.20), $p = 0.025$, respectively. In contrast to ^{18}F-FES, mucinous carcinoma cell type and Allred score of 7–8 were statistically significant with correlation coefficient of 26.65

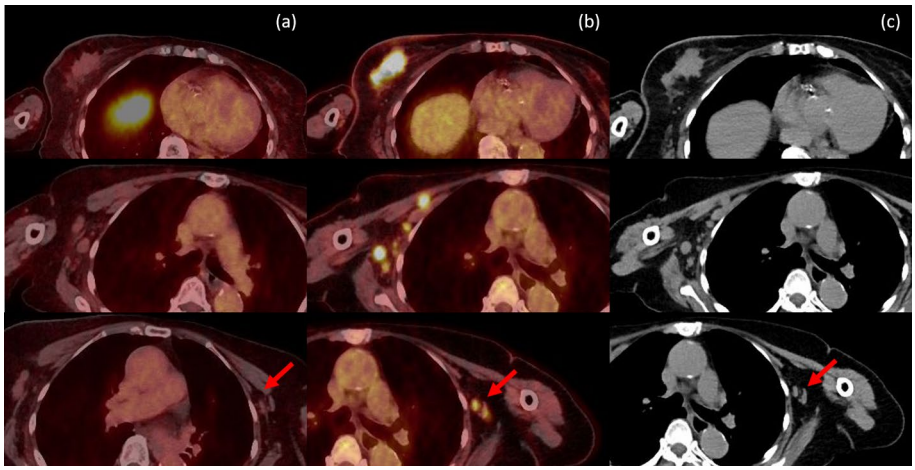

Fig. 4 Fusion PET axial images of ^{18}F-FES **a** and ^{18}F-FDG **b** for ^{18}F-FDG-avid right breast mass and multiple enlarged metastatic nodes at right axilla on CT imaging **c** without ^{18}F-FES avidity, in line with few small ^{18}F-FDG-avid nodes at left axilla (arrow) but no ^{18}F-FES avidity compatible with reactive nodes from recent vaccination and decreased size in follow-up imaging

Table 3 Difference in degree of uptake between ^{18}F-fluorodeoxyglucose and ^{18}F-fluoroestradiol

	Median (interquartile range)		***p*-value**
	^{18}F-flurodeoxyglucose	**^{18}F-fluoroestradiol**	
All lesion			
SUVmax	5.68 (3.41–10.03)	5.38 (2.55–10.60)	0.646
T/N ratio	2.635 (1.58–4.79)	3.335 (1.61–6.38)	0.016
IDC cell type			
SUVmax	6.23 (3.63–10.34)	5.23 (2.29–10.6)	0.138
T/N ratio	3.14 (1.63–5.05)	3.26 (1.55–6.43)	0.144
ILC cell type			
SUVmax	2.15 (1.24–4.25)	4.75 (2.76–8.78)	0.028
T/N ratio	0.96 (0.55–1.79)	3.30 (1.92–6.09)	0.015
Allred score			
SUVmax	4.06 (2.20–6.42)	6.51 (3.51–9.69)	0.003
T/N ratio	1.92 (1.22–2.96)	3.57 (1.97–5.89)	< 0.001
Score < 7			
SUVmax	9.49 (5.22–17.66)	1.72 (1.34–2.79)	< 0.001
T/N ratio	4.96 (3.00–9.37)	1.48 (0.81–2.03)	< 0.001
Luminal Subtype			
Luminal A			
SUVmax	1.92 (1.33–11.13)	3.44 (2.76–6.77)	0.019
T/N ratio	0.86 (0.56–0.96)	2.18 (1.92–3.98)	0.004
Luminal B			
SUVmax	7.39 (3.79–11.13)	5.43 (2.34–10.60)	0.008
T/N ratio	3.56 (1.69–5.05)	3.24 (1.40–6.38)	0.718

IDC Invasive ductal carcinoma, *ILC* Invasive lobular carcinoma, *SUVmax* Maximal standardize uptake value, *T/N ratio* Tumor-to-normal ratio

(95%CI 19.28, 34.02), p-value < 0.001 and 5.90 (95%CI − 0.0005, 11.81), p-value = 0.05, respectively (Table 4).

Discussion

Accurate initial TNM staging is a crucial step for appropriate management and prediction of prognosis in breast cancer (Network 2023). In this study, ^{18}F-FES PET/CT could detect true metastatic lesions better than ^{18}F-FDG PET/CT, as reported by previous studies (Liu et al. 2019; Ulaner et al. 2021; Piccardo et al. 2022; Chae et al. 2020). Our results yielded an overall diagnostic performance of ^{18}F-FES that was comparable to previous studies (Gupta et al. 2017; Piccardo et al. 2022; Chae et al. 2019; Venema et al. 2017; Yang et al. 2013a; Kurland et al. 2020). ^{18}F-FES had remarkably high selective binding to ER. There was no report of any false-positive finding from ^{18}F-FES PET/CT, except one case report of a false-positive from post-radiation pneumonia (Yang

Table 4 Factors associated with degree of uptake in ^{18}F-fluorodeoxyglucose and ^{18}F-fluoroestradiol PET/CT

Factor	^{18}F-fluorodeoxyglucose		^{18}F-fluoroestradiol	
	Correlation coefficient (95% C.I.)	*p*-value	Correlation coefficient (95% C.I.)	*p*-value
Age (year)	0.01 (— 0.14, 0.16)	0.937	0.12 (— 0.08, 0.31)	0.233
BMI (kg/m^2)	0.16 (— 0.37, 0.69)	0.551	0.45 (— 0.21, 1.12)	0.181
Menopause status				
No	Ref		Ref	
Yes	— 0.33 (— 5.30, 4.65)	0.898	5.74 (— 0.54, 12.01)	0.073
Cell type				
Invasive ductal carcinoma	Ref		Ref	
Invasive lobular carcinoma	— 5.32 (— 11.48, 0.84)	0.090	1.46 (— 4.26, 7.19)	0.616
Invasive micropapillary carcinoma	— 0.95 (— 10.24, 8.33)	0.841	— 0.64 (— 8.24, 6.95)	0.868
Mucinous carcinoma	— 5.04 (— 14.18, 4.10)	0.280	26.65 (19.28, 34.02)	< 0.001
Intensity of ER expression				
Weak	Ref		Ref	
Moderate	— 1.87 (— 10.22, 6.48)	0.660	0.34 (— 10.21, 10.90)	0.949
Strong	— 3.82 (— 9.04, 1.40)	0.152	5.83 (— 0.56, 12.22)	0.074
Proportion of ER expression				
< 1%	–		–	
1-10%	Ref		Ref	
11-33%	0.22 (— 10.34, 10.79)	0.967	— 1.33 (— 14.63, 11.96)	0.844
34-66%	— 0.64 (— 8.03, 6.75)	0.865	3.20 (— 6.00, 12.41)	0.495
> 67%	— 2.39 (— 7.87, 3.09)	0.393	5.84 (— 0.75, 12.43)	0.082
Allred Score				
< 7	Ref		Ref	
7–8	— 3.60 (— 8.38, 1.18)	0.140	5.90 (— 0.0005, 11.81)	0.050
Luminal				
A	Ref		Ref	
B	2.76 (1.10, 11.92)	0.018	— 1.39 (— 5.11, 2.34)	0.465
Ki-67	0.11 (0.01, 0.20)	0.025	— 0.06 (— 0.12, 0.01)	0.096

BMI Body mass index, *ER* Estrogen receptor

et al. 2013b), resulting in a remarkably high PPV of 100% in our study. Thus, lesions with ^{18}F-FES uptake were ER-positive metastasis. However, this study showed a low NPV of ^{18}F-FES. This result could be explained by heterogeneity of ER-expression in the tumor with dissimilar expression of ER throughout the whole body (Turashvili and Brogi 2017; Babayan et al. 2013). ^{18}F-FDG PET/CT detects glucose metabolism of tumor cells, with higher uptake in more aggressive tumors. In this study, the diagnostic performance of ^{18}F-FDG PET/CT was also comparable to recent studies (Gupta et al. 2017; Liu et al. 2019; Piccardo et al. 2022; Chae et al. 2020), but lower in specificity and NPV when compared with ^{18}F-FES PET/CT. These findings could be explained by the histological cell type of low-grade breast cancer such as ILC, with false negative in ^{18}F-FDG PET/CT (Kumar et al. 2009) and non-specific uptake of ^{18}F-FDG PET/CT, such as infection and inflammation (Boellaard et al. 2015).

In a subgroup analysis of strong ER-expression (Allred score of 7–8), the diagnostic performance of ^{18}F-FES was improved. Few studies (Gupta et al. 2017; Peterson et al. 2011) yielded good correlation of ^{18}F-FES and ER-expression in breast cancer, with higher ^{18}F-FES uptake in higher ER-expressing tumor cells, resulting in an increased detection rate. In contrast, the diagnostic performance of ^{18}F-FDG PET/CT was worsened due to less aggressive behavior in higher ER-expressing tumor cells (Mooij et al. 2023).

In the patient analysis, ^{18}F-FDG and ^{18}F-FES PET/CT revealed concordant results from TNM stage among 18 of 28 patients (64.29%). Most discordant results were from ^{18}F-FDG PET/CT with 3 false-positive and 5 false-negative cases. Meanwhile, there was only 1 case with false negative ^{18}F-FES PET/CT, showed superiority to ^{18}F-FDG PET/CT for initial staging in ER-positive breast cancer. Interestingly, one case (Fig. 4) was both false-positive in ^{18}F-FDG (contralateral axillary lymph nodes compatible with reactive nodes from recent vaccination that exhibited a decreased size in the follow-up imaging) and false-negative in ^{18}F-FES (primary tumor and regional lymph nodes demonstrated by tissue diagnosis and anatomical findings). Hence, we propose that the combination of ^{18}F-FDG and ^{18}F-FES PET/CT could overcome the limitation of each radiotracer while improving the accuracy for initial staging.

Among semiquantitative parameters, ^{18}F-FES had significantly higher SUVmax and T/N ratio than ^{18}F-FDG PET/CT in lesions of ILC cell type, due to mostly strong ER expression (Xin and Eng 2016), low tumor density, low GLUT-1 expression, low proliferation rates, and infiltrative growth patterns (Fujii et al. 2016). ^{18}F-FES PET/CT also had a significantly higher SUVmax and T/N ratio for Allred score 7–8 and Luminal A subtype. In contrast, ^{18}F-FDG PET/CT had a significant higher SUVmax and T/N ratio in Allred score < 7 and Luminal B subtype. These results could be explained by the difference in the degree of ER-expression and tumor aggressiveness between each group (Peterson et al. 2008; Mooij et al. 2023).

In the multi-linear regression analysis, Allred score 7–8 significantly affected the degree of ^{18}F-FES PET/CT with correlation coefficient of 5.90 (95%CI, − 0.0005, 11.81), $p = 0.05$, whereby higher ER expression was associated with higher ^{18}F-FES uptake. Mucinous carcinoma also significantly affected the degree of ^{18}F-FES uptake. This cell

type usually has low aggressiveness and strong ER-expression (Hashmi et al. 2021), resulting in high ^{18}F-FES uptake. However, this result originated from only one case and further study was recommended. Ki-67 is a marker of cell proliferation with good correlation to the degree of ^{18}F-FDG PET/CT (Tchou et al. 2010) and is a critical criteria for categorize to the Luminal subtype. In our study, Ki-67 and Luminal B subtype were also noted to significantly affect the degree of ^{18}F-FDG PET/CT, with correlation coefficient of 0.11 (95%CI, 0.01, 0.2), $p=0.025$ and 2.76 (95%CI, 1.10,11.92), $p=0.018$, respectively. In this study, BMI and menopause status yielded no significant effect to the degree of ^{18}F-FES uptake, as in previous studies (Venema et al. 2016; Peterson et al. 2011). These results might be mainly due to the menopausal status (78.57%) and the normal BMI (67.86%) of the patients in this study.

Conclusion

The overall diagnostic performance of ^{18}F-FES is comparable to ^{18}F-FDG PET/CT but has better diagnostic performance in Allred score 7–8. The combination of ^{18}F-FDG and ^{18}F-FES PET/CT can overcome the limitation of each radiotracer and improve diagnostic accuracy. Allred score of 7–8 is associated with a higher degree of ^{18}F-FES PET/CT. Meanwhile, there is an association of Ki-67 and luminal B subtype with higher degrees of ^{18}F-FDG PET/CT.

Abbreviations

ER	Estrogen receptor
IHC	Immunohistochemistry
PET/CT	Positron emission tomography/Computed tomography
^{18}F-FDG	^{18}F-Fluorodeoxyglucose
^{18}F-FES	^{18}F-Fluoroestrodiol
BMI	Body mass index
VOI	Voxels of interest
SUVmax	Maximum standardized uptake value
T/N ratio	Tumor-to-normal ratio
MRI	Magnetic resonance imaging
SD	Standard deviation
IQR	Interquartile range
PPV	Positive predictive value
NPV	Negative predictive value
IDC	Invasive ductal carcinoma
ILC	Invasive lobular carcinoma

Acknowledgements

We thank H. Nikki March, PhD, from Edanz (www.edanz.com/ac) for editing a draft of this manuscript.

Author contributions

All authors contributed to the study conception and design. Material preparation, data collection, and data analysis were performed by PK, SM, NH, and AJ. Image interpretation and analysis were performed by PK, CP, AK, DS, and CC. The first draft of the manuscript was written by PK and all authors commented on previous versions of the manuscript. All authors read and approved the final manuscript.

Funding

The authors declare that no funds, grants, or other support was received during the preparation of this manuscript.

Availability of data and materials

The datasets generated during and/or analyzed during the current study are available from the corresponding author on reasonable request.

Declarations

Ethic approval and consent to participate

This study was approved by the Ethics Committee of Chulabhorn Research Institute, EC number 007/2565 and Thai Clinical Trial Registry (TCTR), Trial NumberTCTR20230603002.

Consent for publication

The authors affirm that human research participants provided informed consent for publication of the images.

Competing of interests

The authors declare that they have no competing interests.

Received: 8 August 2023 Accepted: 28 August 2023
Published online: 18 December 2023

References

Amin MB, Edge S, Greene F et al (eds) (2017) AJCC cancer staging manual. Springer, New York
Babayan A, Hannemann J, Spötter J, Müller V, Pantel K, Joosse SA (2013) Heterogeneity of estrogen receptor expression in circulating tumor cells from metastatic breast cancer patients. PLoS ONE 8:e75038
Blamey RW, Hornmark-Stenstam B, Ball G et al (2010) ONCOPOOL - a European database for 16,944 cases of breast cancer. Eur J Cancer 46:56–71
Boellaard R, Delgado-Bolton R, Oyen WJG et al (2015) FDG PET/CT: EANM procedure guidelines for tumour imaging: version 2.0. Eur J Nucl Med Mol Imaging 42:328–354
Chae SY, Ahn SH, Kim SB et al (2019) Diagnostic accuracy and safety of 16α-[18F]fluoro-17β-oestradiol PET-CT for the assessment of oestrogen receptor status in recurrent or metastatic lesions in patients with breast cancer: a prospective cohort study. Lancet Oncol 20:546–555
Chae SY, Son HJ, Lee DY et al (2020) Comparison of diagnostic sensitivity of [18F]fluoroestradiol and [18F]fluorodeoxyglucose positron emission tomography/computed tomography for breast cancer recurrence in patients with a history of estrogen receptor-positive primary breast cancer. EJNMMI Res 10:54
de Mooij CM, Ploumen RAW, Nelemans PJ, Mottaghy FM, Smidt ML, van Nijnatten TJA (2023) The influence of receptor expression and clinical subtypes on baseline [18F]FDG uptake in breast cancer: systematic review and meta-analysis. EJNMMI Res 13:5
Ferlay J, Colombet M, Soerjomataram I et al (2019) Estimating the global cancer incidence and mortality in 2018: GLOBOCAN sources and methods. Int J Cancer 144:1941–1953
Fujii T, Yajima R, Kurozumi S et al (2016) Clinical Significance of 18F-FDG-PET in invasive lobular carcinoma. Anticancer Res 36:5481–5485
Gupta M, Datta A, Choudhury PS, Dsouza M, Batra U, Mishra A (2017) Can 18F-fluoroestradiol positron emission tomography become a new imaging standard in the estrogen receptor-positive breast cancer patient: a prospective comparative study with 18F-fluorodeoxyglucose positron emission tomography? World J Nucl Med 16:133–139
Hashmi AA, Zia S, Yaqeen SR et al (2021) Mucinous breast carcinoma: clinicopathological comparison with invasive ductal carcinoma. Cureus 13:e13650
Kumar R, Rani N, Patel C, Basu S, Alavi A (2009) False-negative and false-positive results in FDG-PET and PET/CT in breast cancer. PET Clin 4:289–298
Kurland BF, Wiggins JR, Coche A et al (2020) Whole-body characterization of estrogen receptor status in metastatic breast cancer with 16α-18F-fluoro-17β-estradiol positron emission tomography: Meta-analysis and recommendations for integration into clinical applications. Oncologist 25:835–844
Liu C, Gong C, Liu S et al (2019) 18F-FES PET/CT influences the staging and management of patients with newly diagnosed estrogen receptor-positive breast cancer: a retrospective comparative study with 18F-FDG PET/CT. Oncologist 24:e1277-1285
Mintun MA, Welch MJ, Siegel BA et al (1988) Breast cancer: PET imaging of estrogen receptors. Radiology 169:45–48
National comprehensive cancer network. Breast cancer (Version 4.2023). https://www.nccn.org/professionals/physician_gls/pdf/breast.pdf. Accessed May 9, 2023
Peterson LM, Mankoff DA, Lawton T, Yagle K, Schubert EK, Stekhova S, Gown A, Link JM, Tewson T, Krohn KA (2008) Quantitative imaging of estrogen receptor expression in breast cancer with PET and 18F-fluoroestradiol. J Nuclear Med 49(3):367–374
Peterson LM, Kurland BF, Link JM et al (2011) Factors influencing the uptake of 18F-fluoroestradiol in patients with estrogen receptor positive breast cancer. Nucl Med Biol 38:969–978
Piccardo A, Fiz F, Treglia G, Bottoni G, Trimboli P (2022) Head-to-head comparison between 18F-FES PET/CT and 18F-FDG PET/CT in oestrogen receptor-positive breast cancer: a systematic review and meta-analysis. J Clin Med 11:1919
Research C for DE and drug trial snapshot: CERIANNA. FDA. https://www.fda.gov/drugs/drug-approvals-and-databases/drug-trial-snapshot-cerianna. Updated Jun 3, 2020. Accessed Jul 8, 2021
Tchou J, Sonnad SS, Bergey MR et al (2010) Degree of tumor FDG uptake correlates with proliferation index in triple negative breast cancer. Mol Imaging Biol 12:657–662
Turashvili G, Brogi E (2017) Tumor heterogeneity in breast cancer. Front Med 4:227
Ulaner GA, Jhaveri K, Chandarlapaty S et al (2021) Head-to-head evaluation of 18F-FES and 18F-FDG PET/CT in metastatic invasive lobular breast cancer. J Nucl Med 62:326
Venema CM, Apollonio G, Hospers GAP et al (2016) Recommendations and technical aspects of 16α-[18F]fluoro-17β-estradiol PET to image the estrogen receptor in vivo: the Groningen experience. Clin Nucl Med 41:844–851
Venema CM, Mammatas LH, Schröder CP et al (2017) Androgen and estrogen receptor imaging in metastatic breast cancer patients as a surrogate for tissue biopsies. J Nucl Med off Publ Soc Nucl Med 58:1906–1912

Weischenfeldt LH, Kirkegaard K, Rasmussen BB et al (2017) A high level of estrogen-stimulated proteins selects breast cancer patients treated with adjuvant endocrine therapy with good prognosis. Acta Oncol Stockh Swed 56:1161–1167
Xin LJJ, Eng LG (2016) A review of invasive lobular carcinoma of the breast: should it be treated like invasive ductal carcinoma? Integr Cancer Sci Therap. https://doi.org/10.15761/ICST.1000211
Yang Z, Sun Y, Zhang Y et al (2013a) Can fluorine-18 fluoroestradiol positron emission tomography-computed tomography demonstrate the heterogeneity of breast cancer in vivo? Clin Breast Cancer 13:359–363
Yang Z, Sun Y, Yao Z, Xue J, Zhang Y, Zhang Y (2013b) Increased (18)F-fluoroestradiol uptake in radiation pneumonia. Ann Nucl Med 27:931–934

Publisher's Note